HHS Public Access

Author manuscript

*Tetrahedron Lett*. Author manuscript; available in PMC 2022 August 03.

Published in final edited form as:

*Tetrahedron Lett*. 2021 August 3; 77: . doi:10.1016/j.tetlet.2021.153248.

# Indoloxytriazines as binding molecules for the JAK2 JH2 pseudokinase domain and its V617F variant

**Ana S. Newton**[a], **Maria-Elena Liosi**[a], **Sean P. Henry**[a], **Luca Deiana**[a], **John C. Faver**[a], **Stefan G. Krimmer**[a,b], **David E. Puleo**[b], **Joseph Schlessinger**[b], **William L. Jorgensen**[a,*]

[a]Department of Chemistry, Yale University, New Haven, Connecticut 06520-8107,

[b]Department of Pharmacology, Yale University School of Medicine, New Haven, CT 06520-8066.

## Abstract

Small molecules that selectively bind to the pseudokinase JH2 domain over the JH1 kinase domain of JAK2 kinase are sought. Virtual screening led to the purchase of 17 compounds among which 9 were found to bind to V617F JAK2 JH2 with affinities of 40 – 300 μM in a fluorogenic assay. Ten analogues were then purchased yielding 9 additional active compounds. Aminoanilinyltriazine **22** was particularly notable as it shows no detectable binding to JAK2 JH1, and it has a 65-μM dissociation constant $K_d$ with V617F JAK2 JH2. A crystal structure for **22** in complex with wild-type JAK2 JH2 was obtained to elucidate the binding mode. Additional *de novo* design led to the synthesis of 19 analogues of **22** with the most potent being **33n** with $K_d$ values of 2–3 μM for WT and V617F JAK2 JH2, and with 16-fold selectivity relative to binding with WT JAK2 JH1.

## Graphical Abstract

*Corresponding author. william.jorgensen@yale.edu.



Declaration of competing Interest

The authors declare no competing interests.

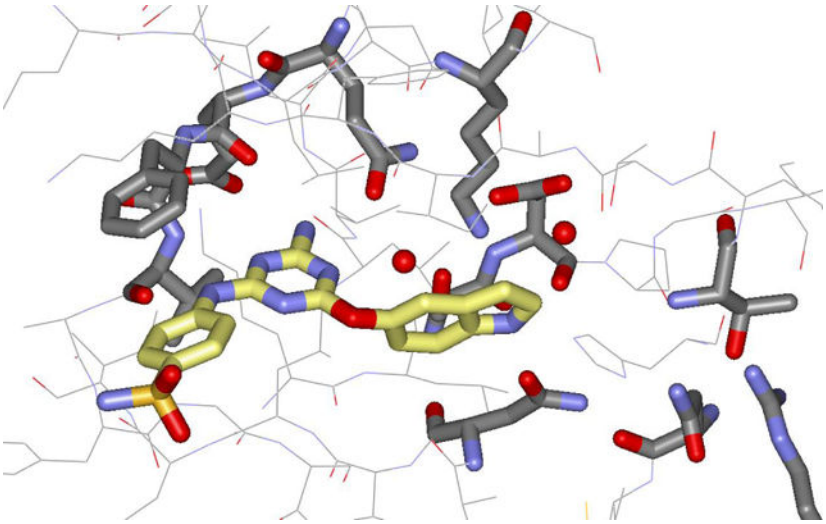

**Keywords**

JAK2 kinase; Pseudokinase domain; JH2/JH1 selectivity; Kinase inhibitors

Irregularities in JAK-STAT signaling pathways are known to cause numerous forms of cancer [1]. The key components of the pathways are Janus kinases (JAKs), the signal transducer and activator of transcription factors (STATs), and cytokine receptors such as erythropoietin or interleukin receptors. Binding of cytokines causes an intracellular signaling cascade featuring phosphorylations by JAKs (JAK1–3 and TYK2), which are multidomain proteins with a C-terminal kinase domain (JH1) and an adjacent pseudo-kinase domain (JH2). Though JH2 domains have an ATP-binding site, they lack the characteristic catalytic aspartate, and they play an essential regulatory role for the JH1 kinase activity. Of particular interest is a single-point mutation, V617F, in the JAK2 JH2 domain, which is responsible for ca. 70% of myeloproliferative neoplasms (MPNs) [2–5]. These conditions including polycythemia vera (PV), essential thrombocythemia (ET), and myelofibrosis (MF) arise from over-production of one or more types of blood cells in bone marrow.

Studies have shown that the hyperactivation caused by the V617F mutation can be reversed by proximal mutations in the JH2 binding site and C helix [6,7]. This coupled with the desire to avoid undesirable side effects associated with inhibition of normal JAK2 JH1 kinase activity, such as thrombocytopenia and anemia, has suggested a small-molecule therapeutic strategy featuring selective binding to the ATP site of JAK2 JH2 [6,8,9]. As an important step in this direction, we have sought to understand the structural features required to achieve strong binding to JAK2 JH2 and simultaneously weak or no binding to the JAK2 JH1domain [10–12].

An initial screen of kinase inhibitors led to identification of JNJ7706621 (**1**) as a strong JAK2 JH2 binder, however, it has a similar ca. 0.5-μM affinity for the JAK2 JH1 ATP-site using a fluorescence polarization assay [10]. Through computer-aided design and crystallography it was possible to evolve this lead into a series of arylamidotriazoles

showing improved binding and selectivity with members such as **2** with $K_d$ values of 0.3 – 0.6 μM with JAK2 JH2 and 6 – 42 μM with JAK2 JH1 [12].

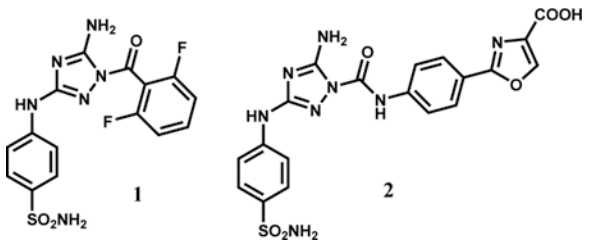


The present work reports on the discovery of an alternative series of JAK2 binding molecules that feature an indoloxytriazine core. This series arose from a virtual screen followed by lead refinement driven by computer-aided design and protein crystallography. Significant challenges are associated with direction of the right-hand substituent as in **2** into the polar ATP-site to achieve JH2/JH1 selectivity and strong binding.

To begin, virtual screening was applied to find molecules that bind to the ATP site in the JH2 domain (Fig. 1). A crystal structure of JAK2 JH2 mutant V617F bound to ATP (PDBID: 4FVR [13]) was used for the protein target. The virtual screen was run using Glide SP [14] with the drug-like subset of the ZINC12 Database, which included more than 10 million compounds (10,637,968) with desirable ADME (absorption, distribution, metabolism and excretion) features [15]. Three hydrogen-bond constraints with Gln626, Glu627 and Val629 were included to provide strong binding to the hinge area.

The best-ranked ca. 6400 compounds were redocked with Glide XP [16], and the ca. 1000 best-scoring complexes were visualized. After additional considerations of potential metabolic labilities, synthetic ease of preparing analogues, and novelty, 17 of the docking hits were purchased. Nine (**3**, **6, 9, 11**–**15, 19**) of the purchased compounds did show binding to JAK2 JH2 V617F with $K_d$ values of 40–300 μM, and five also showed affinity for wild-type (WT) JAK2 JH2 with $K_d$ values of 92–300 μM (Table S1). Furthermore, only three compounds, **5**, **9**, and **15**, exhibited binding with JAK2 JH1. These initial binding affinities were obtained through a fluorescence polarization (FP) assay in which a fluorescently labelled ATP molecule, BODIPY-ATP, was displaced from the JH2 ATP-binding site [10]. The purchase of ten analogues of **13**, **20**–**29**, which were found by substructure search, provided 9 additional active compounds for V617F JAK2 JH2 (Table S1).

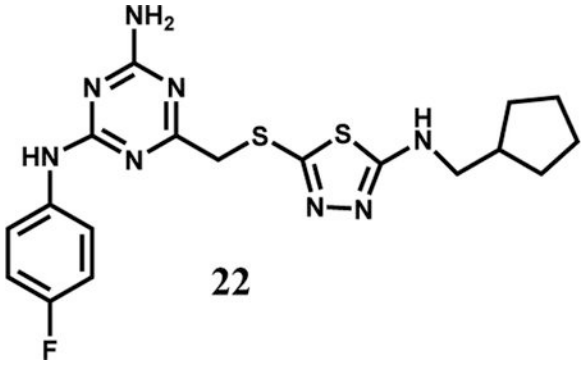


22

Compound **22** was particularly notable as it shows good selectivity with no binding to JAK2 JH1 and $K_d$ values of 149 and 65 μM with WT and V617F JAK2 JH2, respectively. A crystal structure for the WT complex was obtained (Fig. 2A) and confirmed the four expected hydrogen bonds with Gln626, Glu627, and Val629. The thiadiazole-containing appendage, however, bends outward towards the solvent and the electron density for the terminal cyclopentylmethyl group could not be resolved. In order to achieve both selectivity and stronger binding, modifications to grow the ligand to the right towards Thr555 and Arg715 were desired (Fig. 2B) [12]. Modeling of complexes with WT JH2 using MCPRO [17] suggested that replacement of the right-hand substituent with substituted phenoxy groups might suffice, and benefits were also expected from replacing the fluorine atom in **22** with a cyano or sulfamyl group, as in **1** and **2** [12].

Thus, alkylamino, phenoxy analogues **33a–m** of **22** were prepared, as summarized in Scheme 1 and detailed in the ESI. The syntheses featured sequential $S_NAr$ introduction of the anilinyl and aryloxy groups starting from cyanuric chloride or the aminodichlorotriazine. The new compounds reported here are summarized in Table 1. Binding affinities were determined using the updated FP assay with a tracer derived from **1** [11, 12]. The three protein domains, WT JAK2 JH2, V617F JAK2 JH2, and WT JAK2 JH1, were expressed and purified as previously described [10,12].

The SAR was initially explored for the *p*-cyanoanilinyl analogues **33a–f**. The parent phenoxy compound **33a** showed improved binding to WT JAK2 JH2 with a $K_d$ of 73 μM, and addition of a *meta* carboxylate, amino, or hydroxy group brought a two-fold benefit to ca. 40 μM (**33b–d**, Table 1). Fortunately, it was possible to obtain a crystal structure for the complex of **33b** with WT JAK2 JH2 (Fig. 3A); however, it revealed that the phenoxy substituent is again directed outward with one oxygen atom of the *m*-carboxylate group engaged in three hydrogen bonds with the backbone nitrogen (2.79 Å) and hydroxyl oxygen (2.84 Å) of Ser633 and with the hydroxyl oxygen (2.95 Å) of Thr636. This suggested modification of **33d** to increase the acidity of the hydroxyl group by addition of two *ortho* fluorine atoms yielding **33f**. A lower $K_d$ of 10.7 μM did result, though the expectation was that the substituent remained directed outward, as in Figure 3A.

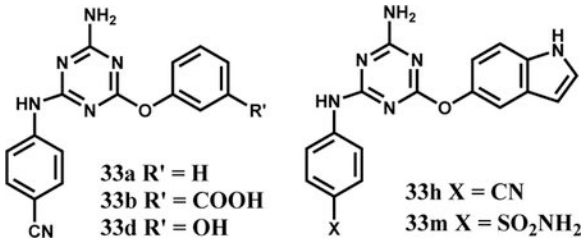


Modeling then considered bicyclic aryloxy possibilities, which led to the notion that a 5-indoloxy substituent might be directed inward to form a hydrogen bond between the indole NH and the sidechain carbonyl group of Asn678. Thus, the cyano and sulfamyl alternatives **33h** and **33m** were synthesized and yielded $K_d$ values of 47 and 18 μM, respectively. Importantly, the structural prediction was confirmed by a crystal structure for **33m** (Fig. 3B). The isomeric indole **33k** and benzimidazole **33l** are less potent, though they are also expected to benefit from cation-π interactions with Lys581 [18].

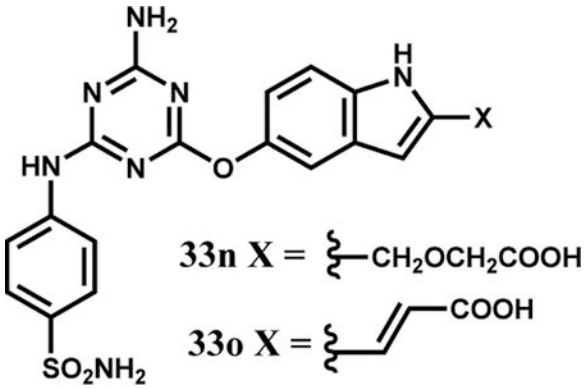


The next step was to further extend the indoles by attachments at C2 to terminate in a carboxylic acid group as in **2** (Fig. 4). This was realized with **33i**, **33j**, **33n**, and **33o**, which did yield the strongest binding molecules at 2–3 μM for WT and V617F JAK2 JH2. The 9- and 17-fold selectivities of **33n** and **33o** for binding the V617F JH2 domain over WT JH1 were also gratifying (Table 1). The right-hand-sides of **33n** and **33o** were synthesized from the common intermediate **37** (Scheme 2), which arose from DIBAL-reduction of the C2-ethyl ester after TBS-protection of the C5-hydroxyl group. Rh(II)-catalyzed etherification of **37** followed by TBAF-deprotection of the silyl group yielded ester **34**, while ester **35** was prepared by oxidation of **37** to the aldehyde, Wittig reaction, and deprotection. The two hydroxyesters underwent $S_NAr$ coupling with anilinylchlorotriazines to yield **33n** directly (the ester hydrolyzed during coupling) and the ester of **33o**, which upon hydrolysis provided the corresponding acrylic acid.

Finally, some modifications of the anilinyl group were considered with **33p–t**, but they did not yield clear binding boosts. The near-equipotency for **33t** and **33m**, however, does provide the 3-amino-5-fluoropyrazole group as a promising *p*-sulfamylaniline surrogate. Additional studies with **33n**, **33o**, and analogues are ongoing. This includes investigation of prodrug strategies to increase permeability for potential testing in cell assays to seek compounds that selectively reduce the hyperactivity of V617F JAK2.

## Supplementary Material

Refer to Web version on PubMed Central for supplementary material.

## Acknowledgments

Gratitude is expressed to the U.S. National Institutes of Health (GM32136) for research support, to the Deutsche Forschungsgemeinschaft (DFG) for a postdoctoral fellowship to S.G.K. (KR 5228/1-1), and to the NIH for training support to D.E.P. (GM007324). This research used resources of the Advanced Photon Source, a U.S. Department of Energy (DOE) Office of Science User Facility operated for the DOE Office of Science by Argonne National Laboratory under contract no. DE-AC02-06CH11357 and also funded by the National Institutes of Health (P30 GM124165) and an NIH-ORIP HEI grant (S10OD021527). This research also used resources of the Yale Macromolecular X-ray Core Facility (NIH grant 1S10OD018007-01). This report is dedicated to Prof. Dale L. Boger with congratulations on his receipt of the Tetrahedron Prize

## References

[1]. Hammarén HM, Virtanen AT, Abraham BG, Peussa H, Hubbard SR, Silvennoinen O, J. Allergy Clin. Immunol143 (2019) 1549–1559. [PubMed: 30092288]

[2]. Baxter EJ, Scott LM, Campbell PJ, East C, Fourouclas N, Swanton S, Vassiliou GS, Bench AJ, Boyd EM, Curtin N, Scott MA, Erber WN, Avis T, Barthorpe A, Bignell G, Blow M, Brackenbury L, Buck G, Clegg S, Clements J, Cole J, Davies K, Edkins S, Gray K, Gorton M, O'Meara S, Halliday K, Harrison R, Haynes W, Hills K, Hunter C, Jones D, Kosmidou V, Laman R, Lugg R, Parker A, Perry J, Petty R, Small A, Solomon H, Stephens P, Stephens Y, Stevens C, Smith R, Tarpey P, Tofts C, Varian J, West S, Widaa S, Bamford S, Butler A, Dawson E, Dicks E, Edwards K, Forbes S, Greenman C, Hinton J, Menzies A, Raine K, Shepherd R, Teague J, Yates A, Wooster R, Futreal A, Stratton M, Green AR, Lancet365 (2005) 1054–1061. [PubMed: 15781101]

[3]. James C, Ugo V, Le Couédic J-P, Staerk J, Delhommeau F, Lacout C, Garçon L, Raslova H, Berger R, Bennaceur-Griscelli A, Villeval JL, Constantinescu SN, Casadevall N, Vainchenker WANature434 (2005) 1144–1148. [PubMed: 15793561]

[4]. Kralovics R, Passamonti F, Buser AS, Teo S-S, Tiedt R, Passweg JR, Tichelli A, Cazzola M, Skoda RC, N. Engl. J. Med352 (2005) 1779–1790. [PubMed: 15858187]

[5]. Levine RL, Wadleigh M, Cools J, Eberts BL, Wernig G, Huntly BJP, Boggon TJ, Wlodarska I, Clark JJ, Moore S, Adelsperger J, Koo S, Lee JC, Gabriel S, Mercher T, D'Andrea A, Fröhling S, Döhner K, Marynen P, Vandenberghe P, Mesa RA, Tefferi A, Griffin JD, Eck MJ, Sellers WR, Meyerson M, Golub TR, Lee SJ, Gilliland DG, Cancer Cell7387–397. [PubMed: 15837627]

[6]. Hammarén HM, Ungureanu D, Grisouard J, Skoda RC, Hubbard SR, Silvennoinen O, Proc. Natl. Acad. Sci. USA112 (2015) 4642–4647. [PubMed: 25825724]

[7]. Leroy E, Balligand T, Pecquet C, Mounton C, Colau D, Shiau AK, Dusa A, Constantinescu SN, J. Allergy Clin. Immunol144 (2019) 224–235. [PubMed: 30707971]

[8]. Leroy E, Constantinescu SN, Leukemia31 (2017) 1023–1038. [PubMed: 28119526]

[9]. Kung JE, Jura NNature Reviews18 (2019) 501–526.

[10]. Puleo DE, Kucera K, Hammarén HM, Ungureanu D, Newton AS, Silvennoinen O, Jorgensen WL, Schlessinger J, ACS Med. Chem. Lett8 (2017) 618–621. [PubMed: 28626521]

[11]. Newton AS, Deiana L, Puleo DE, Cisneros JA, Cutrona KJ, Schlessinger J, Jorgensen WL, ACS Med. Chem. Lett8 (2017) 614–617. [PubMed: 28626520]

[12]. Liosi M-E, Krimmer SG, Newton AS, Dawson TK, Puleo DE, Cutrona KJ, Suzuki Y, Schlessinger J, Jorgensen WL, J. Med. Chem63 (2020) 5324–5240. [PubMed: 32329617]

[13]. Bandaranayake RM, Ungureanu D, Shan Y, Shaw DE, Silvennoinen O, Hubbard SR, Nat. Struct. Mol. Biol19 (2012) 754–760. [PubMed: 22820988]

[14]. Friesner RA, Banks JL, Murphy RB, Halgren TA, Klicic JJ, Mainz DT, Repasky MP, Knoll EH, Shelley M, Perry JK, Shaw DE, Francis P, Shenkin PS, J. Med. Chem47 (2004) 1739–1749. [PubMed: 15027865]

[15]. Irwin JJ, Shoichet BK, J. Chem. Inf. Model45 (2005) 177–182. [PubMed: 15667143]

[16]. Friesner RA, Murphy RB, Repasky MP, Frye LL, Greenwood JR, Halgren TA, Sanschagrin PC, Mainz DT, J. Med. Chem49 (2006) 6177–6196. [PubMed: 17034125]

[17]. Jorgensen WL, Tirado-Rives J, J. Comput. Chem26 (2005) 1689–1700. [PubMed: 16200637]

[18]. Turupcu A, Tirado-Rives J, Jorgensen WL, J. Chem. Theory Comput16 (2020) 7184–7194. [PubMed: 33048555]

- Aberrant increase in JAK2 kinase activity causes myeloproliferative disorders
- Selective binding to the JAK2 pseudokinase domain JH2 may be deactivating
- Small molecules that selectively bind JH2 over the JH1 kinase domain are reported
- The best binding molecules have an indoloxytriazine core


**Figure 1.**
Virtual screening protocol.

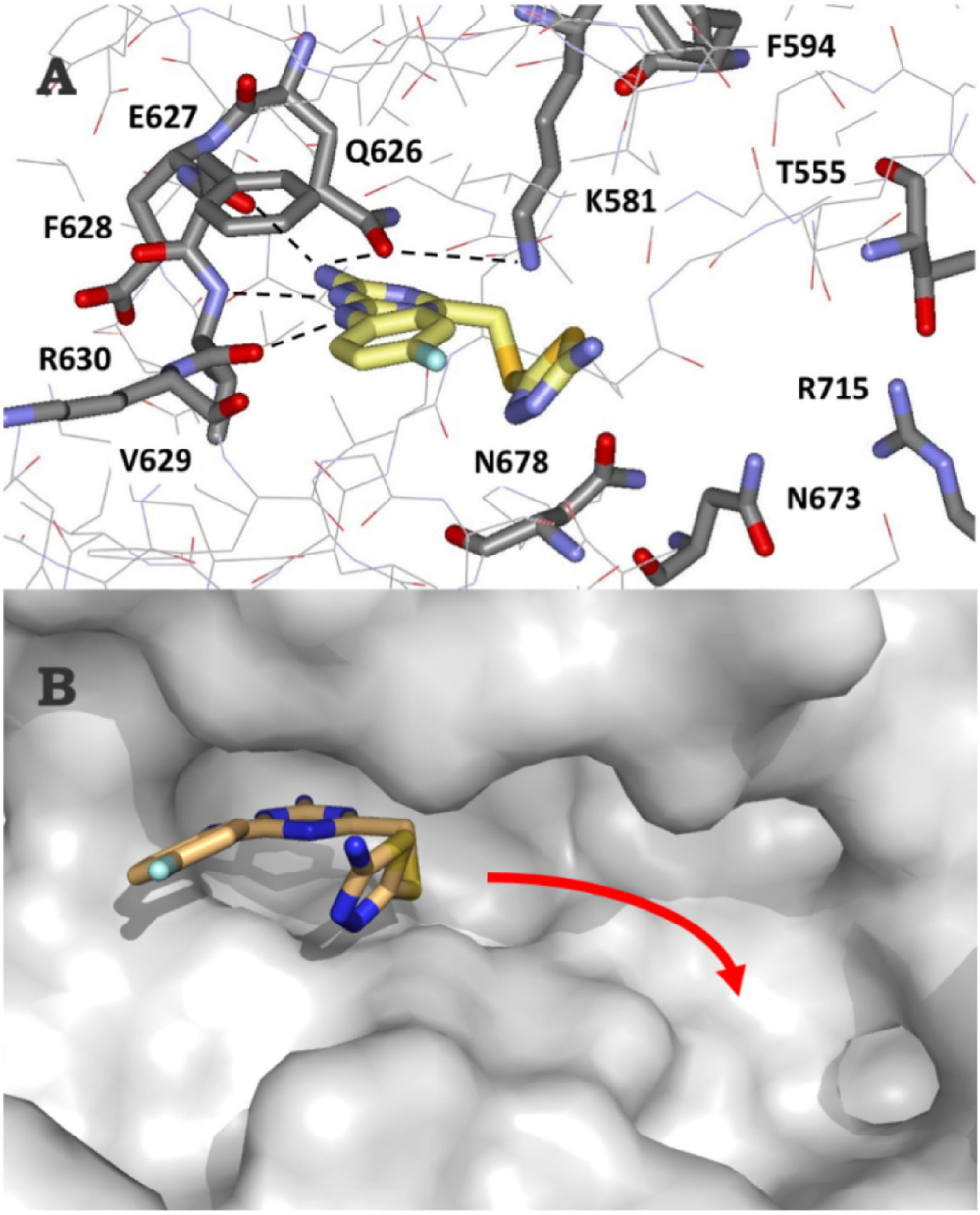


**Figure 2.**

(**A**) Rendering from the 1.86-Å crystal structure of **22** with wild-type JAK2 JH2 (PDB ID 7JYQ). Orientation of **22**, with hydrogen bonds in the hinge area dashed. (**B**) Desired direction of growth in the ATP-binding pocket is indicated with the red arrow.

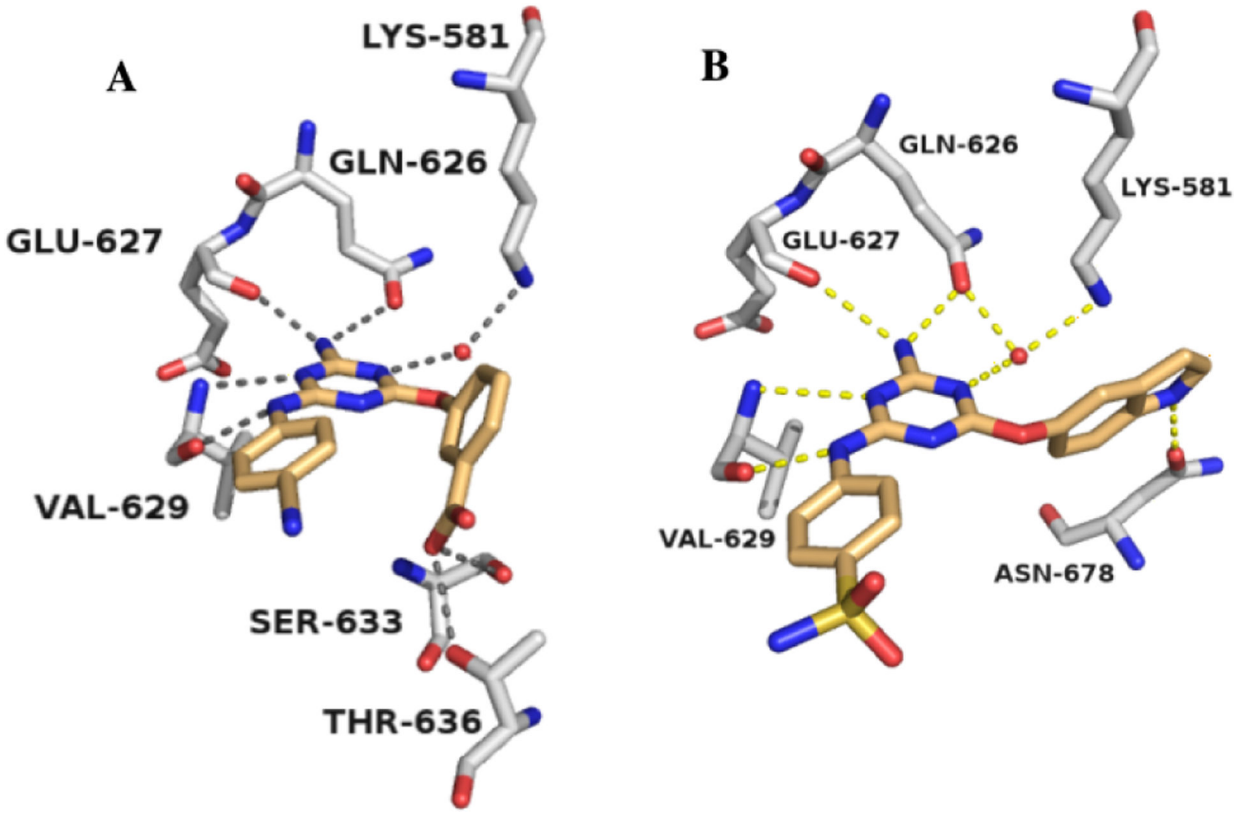


**Figure 3.**

Renderings from the (**A**) 2.16-Å crystal structure of **33b** (PDB ID 7JYO) and (**B**) 2.02-Å crystal structure of **33m** (PDB ID 6XJK) with wild type JAK2 JH2.

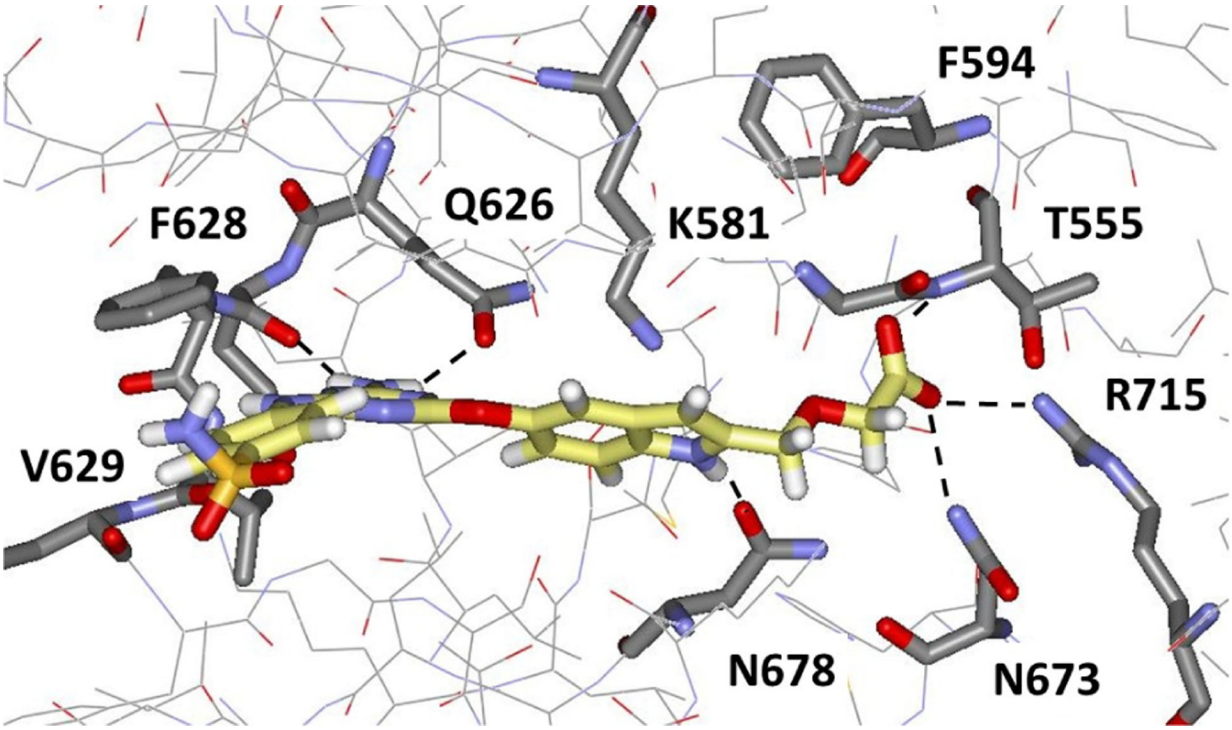


**Figure 4.**

Computed structure using MCPRO [17] for **33n** with WT JAK2 JH2 illustrating the expected eastward extension towards Arg715.

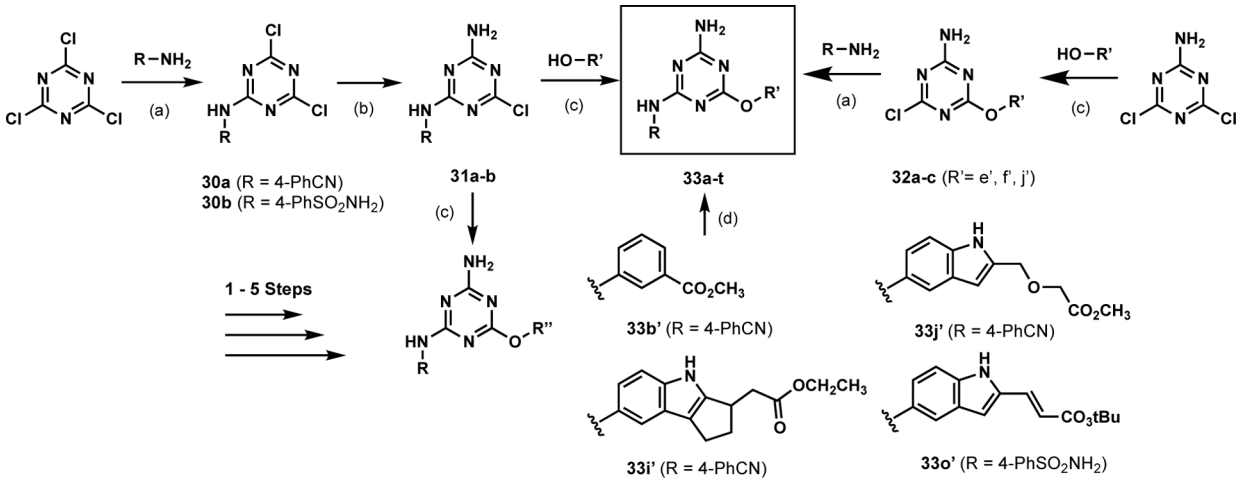


**Scheme 1.**

General synthetic scheme for anilinylaryloxytriazines.[a]

[a] Reagents and conditions: (a) $K_2CO_3$, Acetone, 0 → 23 °C; or $K_2CO_3$, DMF, 70 °C, 10–86 % yield (b) $NH_4OH$ (28%), Acetone, 0 → 23 °C, 71–85 % yield (c) $K_2CO_3$, Acetone, 0 → 23 °C; or $K_2CO_3$, DMF, 60–70 °C, 12.5–68 % yield (d) 2M NaOH (aq) or TFA, THF or EtOH, or dioxane, or $CH_2Cl_2$.

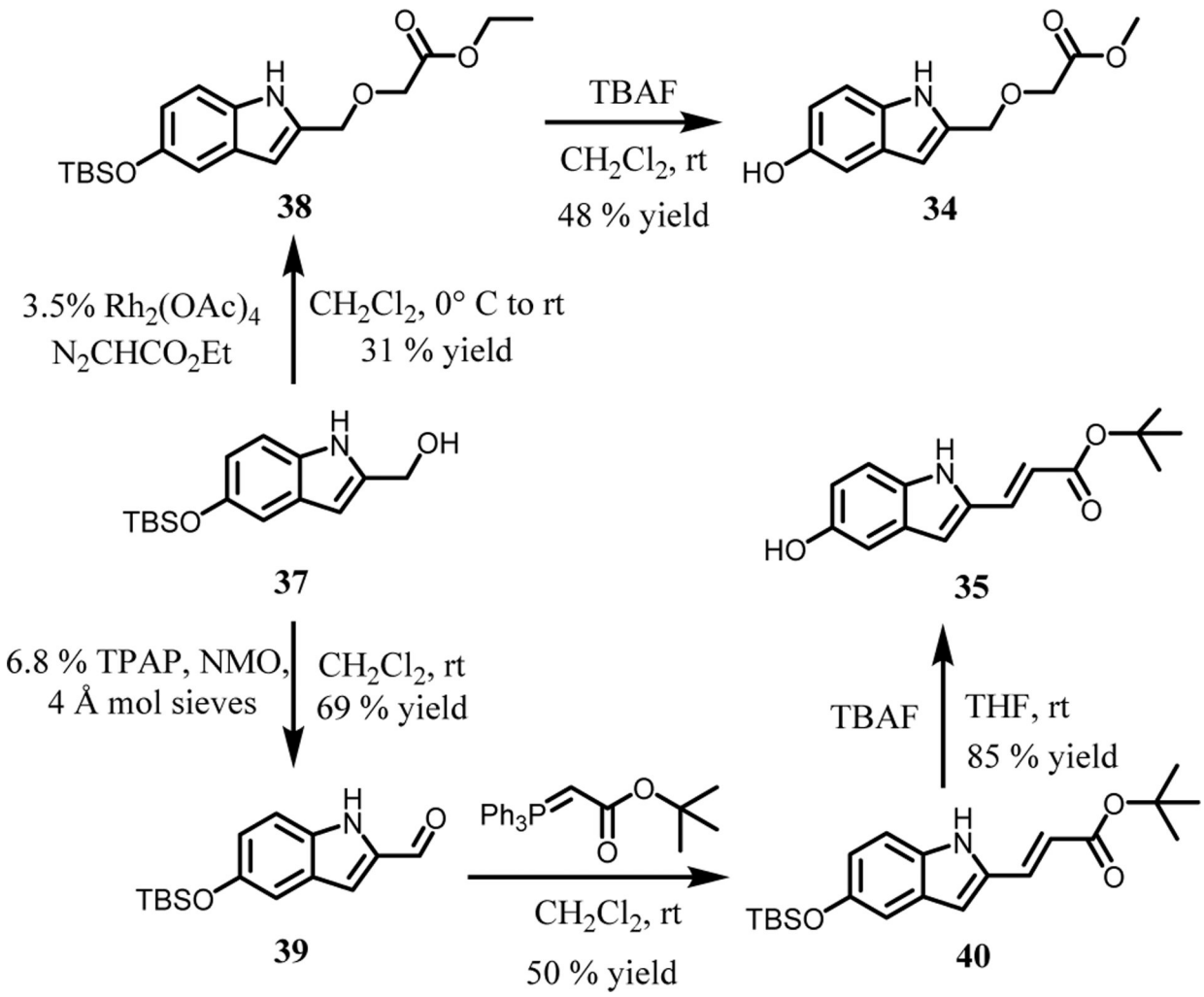


**Scheme 2.**
Synthetic scheme for substituted indoles.

*Tetrahedron Lett*. Author manuscript; available in PMC 2022 August 03.

**Table 1.**

Compounds (**33**) and their experimental binding affinities ($K_d$) using the fluorescence polarization (FP) assay [11].

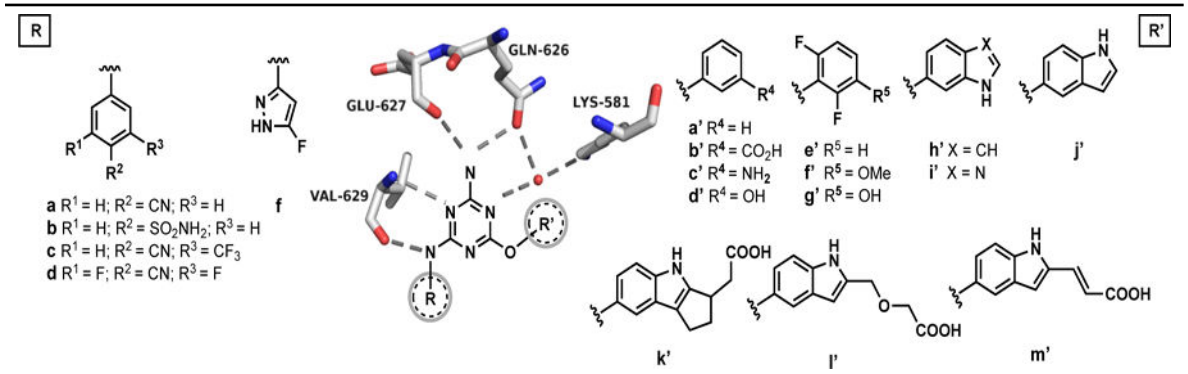


| Compound | R | R' | $K_d$ (μM) | | |
|---|---|---|---|---|---|
| | | | JAK2 JH1 | JAK2 JH2 WT | JAK2 JH2 V617F |
| **33a** | a | a' | | 73.4 ± 20.3 | |
| **33b** | a | b' | | 39.6 ± 3.2 | |
| **33c** | a | c' | | 40.7 ± 4.9 | |
| **33d** | a | d' | | 43.8 ± 12.2 | |
| **33e** | a | f' | | 17.4 ± 9.1 | |
| **33f** | a | g' | | 10.7 ± 1.9 | |
| **33g** | a | h' | | 34.9 ± 1.5 | |
| **33h** | a | J' | | 47.4 ± 6.9 | |
| **33i** | a | k' | | 14.0± 1.0 | |
| **33j** | a | l' | ND (15% @ 50 μM) | 5.9± 0.7 | 4.3± 0.1 |
| **33k** | b | h' | | 20.9 ± 9.2 | |
| **33l** | b | i' | | 31.6± 5.7 | |
| **33m** | b | J' | ND (16% @ 50 μM) | 18.3 ± 3.3 | 8.0± 0.8 |
| **33n** | b | l' | 41.1 ± 7.8 | 2.6 ± 0.1 | 2.4 ± 0.4 |
| **33o** | b | m' | 18.0± 2.7 | 3.3± 1.2 | 2.0± 0.1 |
| **33p** | c | J' | | 53.5 ± 17.9 | |
| **33q** | d | J' | | ND (15% @ 50 μM) | |

| Compound | R | R' | $K_d$ (μM) | | |
|---|---|---|---|---|---|
| | | | JAK2 JH1 | JAK2 JH2 WT | JAK2 JH2 V617F |
| **33r** | f | e' | | 122.7 ± 22.0 | |
| **33s** | f | f' | | 54.7 ± 12.2 | |
| **33t** | f | J' | | 23.2 ± 1.4 | |
| **JNJ7706621 (1)** | | | 0.671 ± 0.175 | 0.456 ± 0.124 | 0.599 ± 0.087 |